Journal of Solid State Chemistry 183 (2010) 1473–1476

Contents lists available at ScienceDirect

Journal of Solid State Chemistry

journal homepage: www.elsevier.com/locate/jssc

Rapid Communication

Structure and magnetic properties of $AgFeP_2O_7$

Kateryna V. Terebilenko [a,*], Alexander A. Kirichok [a], Vyacheslav N. Baumer [b], Maksym Sereduk [a], Nikolay S. Slobodyanik [a], P. Gütlich [c]

[a] Inorganic Chemistry Department, Kiev University, Volodimirska Street 64, Kiev 01601, Ukraine
[b] STC "Institute for Single Crystals" NAS of Ukraine, 60 Lenin ave., Kharkiv 61001, Ukraine
[c] Institut für Anorganische und Analytische Chemie, Johannes-Gutenberg-Universität, Staudinger-Weg 9, D-55099 Mainz, Germany

ARTICLE INFO

Article history:
Received 22 March 2010
Accepted 31 March 2010
Available online 8 April 2010

Keywords:
Silver
Pyrophosphate
Antiferromagnetism
Flux synthesis
IR-spectroscopy

ABSTRACT

$AgFeP_2O_7$ has been synthesized by flux crystallization and characterized by single crystal and powder X-ray diffraction (sp. gr. $P2_1/c$, $a=7.3298(2)$, $b=7.9702(2)$, $c=9.5653(2)$ Å, $\beta=111.842(1)^\circ$, $V=518.68(2)$ Å^3) and FTIR-spectroscopy. The structure is composed of isolated iron octahedra and phosphate tetrahedra interconnected into 3D network with hexagonal channels, where silver counterions are located. The magnetic behavior of the compound approaches the Curie–Weiss equation with a Weiss constant $\theta=-165.9$ K indicating strong antiferromagnetic interaction between iron(III) ions.

1. Introduction

Investigation of complex iron phosphates has revealed a large family of compounds containing high-spin iron(III). Most attention has been paid to the magnetic behaviour of such compounds due to its perspective application as magnetic materials [1]. From structural and magnetic point of view, two possible ways of interaction can occur between iron centres leading to strong magnetic exchange. The first one occurs through an oxygen atom, while the second one is weaker and is realised via a bridging phosphate group. For example, antiferromagnetic coupling as well as weak ferromagnetism below the ordering temperature was observed previously for a series of solid solutions $Li_{1-3x}Fe_xNiPO_4$ ($x=0$–0.15) [2] and $Li_3Fe_2(AsO_4)_{3-x}(PO_4)_x$ ($x=0, 1, 1.5, 2$) [3] with a structural fragment Fe–O–Fe. Exchange path Fe–O–P–O–Fe is responsible for the antiferomagnetic ordering as it was found in α-$Li_3Fe_2(PO_4)_3$ [4] and $K_{11}Fe_{15}(PO_4)_{18}O$ [5].

Among others, five pyrophosphates with the general formula $M^IFeP_2O_7$ (M^I=Li–Cs) were synthesized and their magnetic behaviour was investigated [6–8]. All compounds except the lithium-containing analogue crystallized in the same space group $P2_1/c$. Although their rigid frameworks are built up in a similar way involving infinite rows of isolated FeO_6 octahedra linked by the pyrophosphate bridges, different magnetic properties have been pointed out in a number of works [8,10,11]. It is known, that the magnetic behaviour of magnetically active compounds strongly correlates with structural features, for example, with the local environment of paramagnetic centers and their nearest neighbours. In pyrophosphates the change of the alkali metal by a more voluminous analogue or even substitution of it by *d*-metal can result in distortion of iron coordination sphere because of difference in radii and different electronic structure of the ions. Both effects can influence the magnetic properties of compounds.

Herein synthesis, crystal structure and magnetic behaviour of a new silver-containing member of $M^IFeP_2O_7$ family are presented.

2. Experimental

2.1. Synthesis

The single crystals of $AgFeP_2O_7$ were prepared by the flux growth method. 1.40 ml of H_3PO_4 (14 mol/l) was added dropwise to a ground mixture of 5.00 g of $AgNO_3$ and 0.87 g of Fe_2O_3 in a silica crucible. The mixture was preheated until total decomposition of the initial ingredients. Then the crucible was rapidly heated up to 1000 °C. The obtained melt was kept at this temperature for 1 h to dissolve Fe_2O_3. Afterwards it was cooled to 900 °C at a rate of 50 °C/h and finally to 750 °C at 15 °C/h. The crystalline products, peach-colored rods with typical length 2 mm, were leached out with 25%-ammonia solution to dissolve the vitreous residue (60% yield). Powder XRD study confirmed $AgFeP_2O_7$ monophase.

2.2. X-ray diffraction

The structure was determined from single-crystal X-ray diffraction data obtained using an Oxford Diffraction XCalibur-3

* Corresponding author.
E-mail address: Tereb@bigmir.net (K.V. Terebilenko).

0022-4596/$ - see front matter © 2010 Elsevier Inc. All rights reserved.
doi:10.1016/j.jssc.2010.03.042

diffractometer equipped with 4 MPixel CCD detector. It was solved using direct methods with SHELXS-97 [12] and refined using full-matrix least-squares technique in anisotropic approximation with SHELXL-97 [13]. The heavy atoms were located directly, whereas the remaining oxygen atoms were found using difference Fourier maps calculated during refinement.

Crystal data and refinement are listed in Tables 1 and 2 and selected geometric parameters in Table 3. Further details of the crystal structure investigations can be obtained from the Fachinformationszentrum Karlsruhe, 76344 Eggenstein-Leopoldshafen, Germany (fax: +49 7247 808 666; e-mail: crysdata@fizkarlsruhe.de) on quoting the depository number CSD-421113.

Powder pattern was collected using a Siemens D500 diffractometer (Cu$K\alpha$ radiation, $\lambda=1.54184$ Å; curved graphite monochromator on the counter arm; $2^\circ \le 2\theta \le 100^\circ$, scan step 0.02°, dwell time 40 s). The structure model from single crystal experiment was employed for the Rietveld refinement of powder data. Strong preferred orientation and microabsorption effects were revealed and taken into account. Final agreement indexes are follows: $R_p=7.30\%$, $R_{wp}=9.52\%$, $\chi^2=5.26\%$, $R_{Bragg}=8.15\%$, $R_F=4.00\%$. Refined triclinic cell dimensions: $a=7.3298(2)$ Å, $b=7.9702(2)$ Å, $c=9.5653(2)$ Å, $\beta=111.842(1)^\circ$, $V=518.68(2)$ Å^3. Results of Rietveld refinement are shown in Fig. 1.

Table 1
Crystallographic data and structure refinement parameters of $AgFeP_2O_7$.

Formula unit	$AgFeP_2O_7$
Formula weight	337.66
Crystal system	Monoclinic
Space group	$P2_1/c$ (no. 14)
Cell parameters	
a (Å)	7.33380(10)
b (Å)	7.97310(10)
c (Å)	9.5665(2)
V (Å^3)	519.296(15)
Z	4
β	111.823(2)
ρ_{cal} (g cm^{-1})	4.319
Intensity measurements	
Crystal dimensions (mm^3)	$0.1\times0.07\times0.05$
Apparatus	XCalibur-3 CCD
Wavelength (Å)	(Mo$K\alpha$)=0.71073
Monochromator	Graphite
μ (mm^{-3});	7.162
Scan mode	φ and ω scans
Theta range	2.99–29.99°
Unique reflections, R_{int}	1518, 0.023
h_{range}	$-10\rightarrow6$
k_{range}	$-11\rightarrow11$
l_{range}	$-13\rightarrow13$
Structure solution and refinement	
Weighting scheme	$w=1/[\sigma(F_o^2)+(0.0599P)^2+5.7323P]$, where $P=(F_o^2+2F_c^2)/3$
Absorption correction; T_{min}, T_{max}	Integration 0.566, 0.5963
Resolution method	Heavy atom method
Agreement factors	$R_1=0.0373$; w$R=0.111$; $S=1.13(F_o>2\sigma F_o)$
Number of parameters	101
$(\Delta\rho)_{max,\ min}$ (e/Å^{-3})	1.905, −2.227

Table 2
The coordinates and isotropic thermal parameters of the atoms for $AgFeP_2O_7$.

Atom	Site	x	y	z	U_{ani} (Å^2)
Ag1	4e	0.79388 (7)	0.52615 (6)	0.30987 (6)	0.02271 (19)
Fe1	4e	0.23958 (9)	0.49152 (8)	0.24940 (7)	0.00338 (18)
P1	4e	0.17419 (16)	0.79125 (14)	0.45374 (12)	0.0024 (2)
P2	4e	0.57436 (16)	0.74658 (13)	0.45575 (12)	0.0022 (2)
O1	4e	0.0341 (5)	0.9147 (4)	0.3472 (4)	0.0069 (6)
O2	4e	0.1868 (5)	0.8030 (4)	0.6146 (4)	0.0063 (6)
O3	4e	0.3814 (5)	0.8468 (4)	0.4461 (4)	0.0069 (6)
O4	4e	0.1400 (5)	0.6101 (4)	0.3977 (4)	0.0055 (6)
O5	4e	0.5076 (5)	0.5880 (4)	0.3603 (4)	0.0052 (6)
O6	4e	0.6912 (5)	0.7094 (4)	0.6194 (4)	0.0081 (6)
O7	4e	0.6822 (5)	0.8660 (4)	0.3927 (4)	0.0075 (6)

Table 3
Selected bond lengths (Å) and bond angles (deg) for $AgFeP_2O_7$ structure.

FeO_6 polyhedra					
Fe–O(1)	1.969 (4)	Fe–O(4)	2.052 (4)	Fe–O(6)	1.981 (3)
Fe–O(2)	2.031 (3)	Fe–O(5)	2.008 (4)	Fe–O(7)	1.939 (4)
P_2O_7 group and Ag–Ag distance					
P(1)–O(1)	1.511 (3)	P(2)–O(3)	1.598 (4)	P(2)–O(3)–P(1)	133.66 (26)
P(1)–O(2)	1.510 (4)	P(2)–O(5)	1.530 (3)	Ag–Ag	3.791 (5)
P(1)–O(3)	1.610 (4)	P(2)–O(6)	1.509 (4)		
P(1)–O(4)	1.529 (3)	P(2)–O(7)	1.500 (4)		

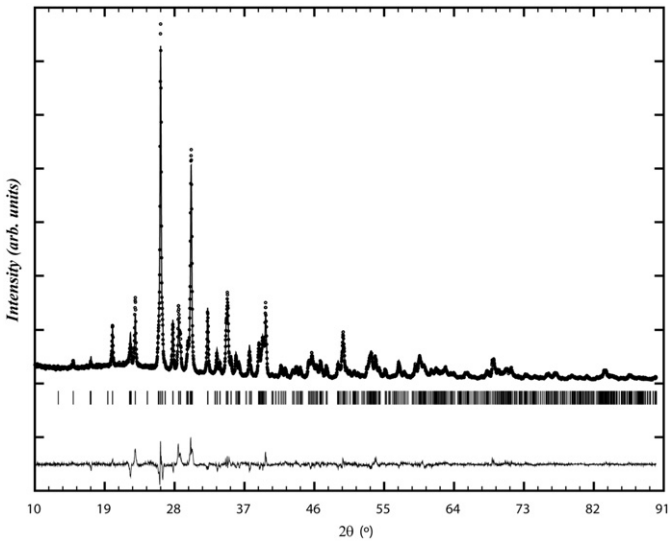

Fig. 1. Powder X-ray diffraction pattern and Rietveld analysis for $AgFeP_2O_7$ and (circle signs correspond to observed data; the solid line is the calculated profile; tick marks represent the positions of allowed reflection and a difference curve on the same scale is plotted at the bottom of the pattern).

2.3. FTIR-spectroscopy, differential thermal analysis and magnetic measurements

FTIR spectroscopy: The FTIR-spectrum was studied in the range of 400–1500 cm^{-1} and collected at a room temperature in KBr discs using a NICOLET Nexus 470 (FTIR) spectrometer.

Differential thermal analysis (DTA) was carried out on a Quasy-1500 thermal analyzer in the temperature range 20–1100 °C (heating rate 5°/min). The experiments were performed on a ground powder of selected single crystals of $AgFeP_2O_7$.

Magnetic measurements: Variable-temperature magnetic susceptibility measurements were recorded with a Quantum Design MPMS2 SQUID susceptometer equipped with a 7 T magnet, operating at temperatures in the range 2–400 K. The susceptometer was calibrated with metallic palladium. Measurements were performed on the finely ground sample (15–30 mg). The magnetic data were corrected for the sample holder and the diamagnetic contribution.

3. Results and discussion

Among possible synthetic ways of silver phosphates preparation flux technique plays a secondary role in comparison with solid state reaction due to difficulties related to the determination of the acceptable ratio of the initial components. Taking into account relatively low basicity of silver in comparison with sodium, the ratio M^I/P in melt was increased from 0.9 to 1.2 ($NaFeP_2O_7$ synthesis [14]) up to 1.5–2.0 (5–10 mol% Fe_2O_3 in a charge), which led to formation of single crystals of silver iron pyrophosphate.

Anion identification was performed by FTIR spectrum analyzing (Fig. 2) that is rather typical for pyrophosphates. Two singlet bands centered at 729 and 940 cm^{-1} are attributed to symmetric (ν_s) and asymmetric (ν_{as}) P–O–P vibrational modes, respectively. Wide multiplet in the range of 1036–1254 cm^{-1} corresponds to ν_3(P–O) vibrational mode. The O–P–O bending vibration (ν_4) is represented by a triplet in the 515–592 cm^{-1} region.

TGA studies indicate no weight loss up to 1000 °C; however, above this temperature the sample loses weight continuously that corresponds to evaporation of some volatile components due to decomposition. The total weight loss at 1100 °C is 4.3 mass%. In contrast to $KFeP_2O_7$ having multiple phase transitions at 180, 428 and 480 °C [18], silver analogue exhibits only an endothermic peak at 1000 °C due to melting. At 1100 °C the sample originates two-layered liquid: the heaviest one contains metallic silver with the topping of a vitreous bulk due to a possible scheme of decomposition:

$$4AgFeP_2O_7 = 4Ag + O_2 + Fe_4P_8O_{26(glassy)}$$

The weight loss is somewhat lower than the calculated value (4.7 mass% provided by the scheme above) indicating incomplete decomposition.

$AgFeP_2O_7$ is isostructural to $M^IFeP_2O_7$ (M^I=Na, K, Rb, Cs) double phosphates family [8–11]. Its framework is built up from infinite rows of isolated iron octahedra connected to five P_2O_7 groups, one of them acting as a "chelating" sequence around the transition metal (Fig. 3). As a result of these blocks' assemblage 3D-framework is formed with hexagonal tunnels, where silver cations reside (Fig. 4). Fe–O bonds in FeO_6-octhahedra lie in the range of 1.93–2.05 Å and the same was also observed for sodium analogue [8] (Table 3). The diphosphate group contains two distorted PO_4 tetrahedra in staggered conformation, with long P–O bonds to the bridging O atom and shorter bonds to the terminal O atoms.

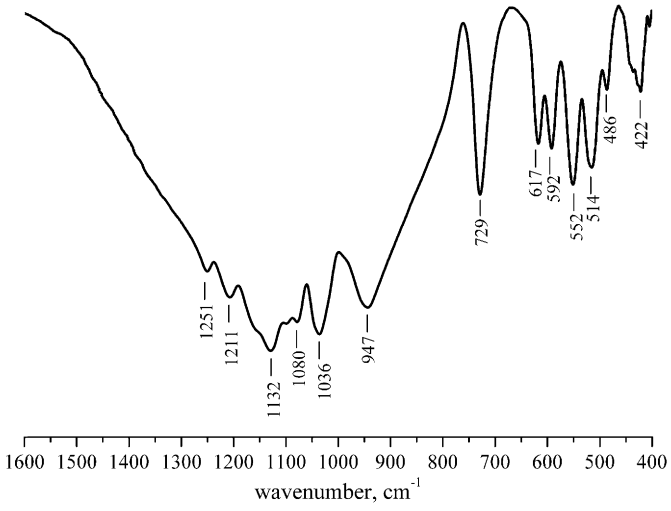

Fig. 2. FTIR-spectrum of $AgFeP_2O_7$.

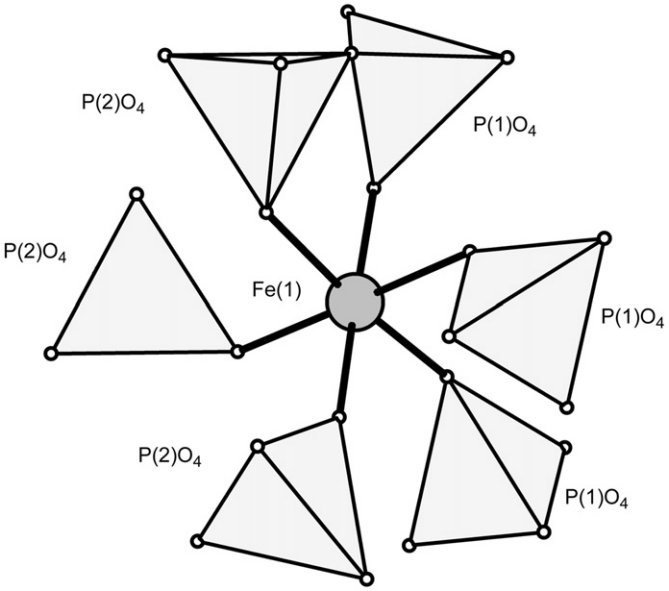

Fig. 3. Association mode involved by iron octahedra and phosphate tetrahedra.

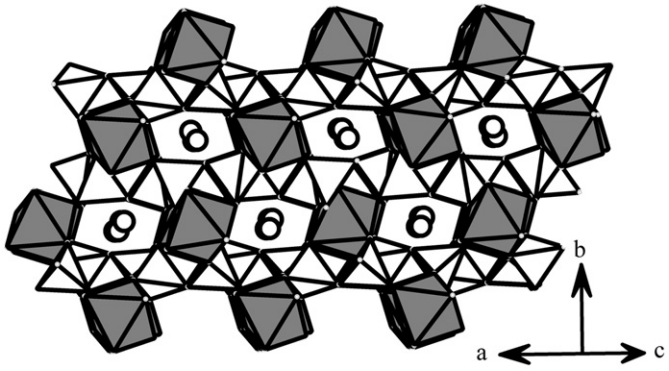

Fig. 4. Formation of hexagonal channels filled by silver atoms in the structure.

Table 4
Comparison of some structural and magnetic data for a series of $M^IFeA_2O_7$ (M^I=Li, Na, K, Cs, Ag, A–P, As).

Compound	Pr. gr.	Z	< A–O–A	Θ (K)	Ref.
$LiFeP_2O_7$	$P2_1$	2	129.6 (2)	−73	[8]
$NaFeP_2O_7$	$P2_1/c$	4	132.86	−53	[9]
$KfeP_2O_7$	$P2_1/c$	4	124.32	−90	[16]
$CsFeP_2O_7$	$P2_1/c$	4	128.47	−64.9	[16]
$AgFeP_2O_7$	$P2_1/c$	4	133.66	−165.9	This work
$KFeAs_2O_7$	P-1	4	116.99 119.20	−41.5	[15]

Substitution of alkali metal by lithium [8] or P_2O_7 on As_2O_7 [15] leads to decrease of cell symmetry but in both cases FeO_6 is surrounded by six pyrophosphate groups. This fact can be explained by high flexibility of $[FeP_2O_7]^-$ network toward counterion (Na, K, Rb, Cs, Ag) due to adaptable bond angles of P–O–P (Table 4). In case of lithium substitution structural changes

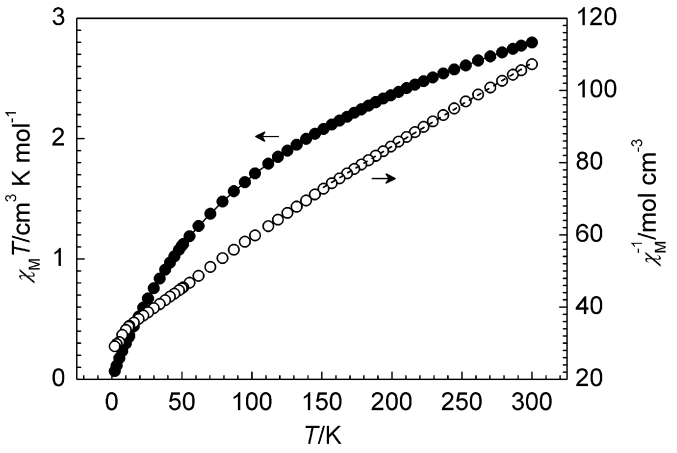

Fig. 5. Plot of $\chi_M T$ and χ_M^{-1} versus T for $AgFeP_2O_7$.

appear due to a small radius and high polarization capacity, while the pyroarsenate derivative crystallizes in a triclinic system specified by more rigid bridges As–O–As. These structural changes determine the magnetic behavior of $M^IFeA_2O_7$ compounds (M^I=Li, Na, K, Cs, Ag, A–P, As).

The magnetic susceptibility of $AgFeP_2O_7$ was measured in the 2–300 K range at 200 Oe by using a polycrystalline powder sample (Fig. 5). The linear behavior of $\chi_M^{-1}(T)$ above 150 K obeys well the Curie–Weiss equation with a Weiss constant $\theta = -165.9$ K, thus indicating an overall strong antiferromagnetic interaction. The value of $\chi_M T$ at 300 K is 2.79 $cm^3\,K\,mol^{-1}$ is much less than the spin-only value of 4.38 $cm^3\,K\,mol^{-1}$ expected for a magnetically isolated high-spin Fe^{III} ion. The product $\chi_M T$ decreases smoothly to zero at 2.0 K. Drop of $\chi_M T$ in the low temperature region could origin also from zero-field splitting of the $S=\frac{5}{2}$ ground state.

Compounds $M^IFeA_2O_7$ (M^I=Li, Na, K, Cs, Ag, A–P, As) represent different magnetic behavior mostly due to structural features (Table 4). Thus, the magnetic susceptibility for isostructural analogues (M^I=Na, K, Cs, Ag, A–P) shows similar linear behavior in the range 50–150 K, while $KFeAs_2O_7$ [15] as well as $LiFeP_2O_7$ shows generally the same temperature dependence but with ferromagnetic contribution [15,17]. Within the group of compounds with space group $P2_1/c$ (M^I=Na, K, Cs) Weiss constants are comparable: its value goes up with the decrease of P–O–P angle. In this sense the compound $AgFeP_2O_7$ stands out with a much higher value of the Weiss constant. This fact might be explained by an efficient mediation of exchange interactions between iron centers via the path Fe–O–Ag–O–Fe, particularly by the involvement of the *d*-orbitals of silver ions. To the best of our knowledge the role of the silver in magnetic properties of phosphates was not reported and analyzed before, partially due to lack of magnetic data for this type of compounds.

4. Conclusion

The family of $M^IFeP_2O_7$ (M^I=alkaline metal) has been extended by a new member $AgFeP_2O_7$. It was shown that substitution of an alkaline metal by silver does not affect significantly the geometry of the framework, but nevertheless slight deviations of P–O–P angle have been observed when compared with those of analogues. These changes have been reflected on the magnetic behavior of the title compound. Although all compounds of the series show antiferromagnetic behavior, the Weiss constant of $AgFeP_2O_7$ is shifted to a substantially lower value in comparison with that of other members.

Acknowledgments

We thank Dr. Igor O. Fritsky and Igor V. Zatovsky (Inorganic Chemistry Department, Kiev University) for useful discussion and the ICDD for financial support (Grant ♯03-02).

Appendix A. Supplementary material

Supplementary data associated with this article can be found in the online version at doi:10.1016/j.jssc.2010.03.042.

References

[1] D. Maspoch, D. Ruiz-Molina, J. Veciana, Chem. Soc. Rev. 36 (2007) 770.
[2] A. Goni, L. Lezama, M.I. Arriortua, G.E. Barberis, T. Rojo, J. Mater. Chem. 10 (2000) 423.
[3] J.L. Mesa, A. Goni, A.L. Brandl, N.O. Moreno, G.E. Barberis, T.J. Rojo, Mater. Chem. 10 (2000) 2779.
[4] J.L. Zarestky, D. Vaknin, B.C. Chakoumakos, T.J. Rojo, A. Goni, G.E. Barberis, J. Magn. Magn. Mater. 234 (2001) 401.
[5] B. Lajmi, M. Hidouri, A. Wattiaux, L. Fourne, J. Darriet, M.J. Ben Amara, Alloys Compd. 361 (2003) 77.
[6] E.A. Genkina, B.A. Maksimov, V.A. Timofeeva, A.B. Bykov, Dokl. Akad. Nauk SSSR 284 (1985) 864.
[7] D. Riou, Ph. Labbe, M. Goreaud, Eur. J. Solid State Inorg. Chem. 25 (1988) 215.
[8] T. Moya-Pizarro, R. Salmon, L. Fournes, Le Flem, G. Wanklyn, B.P. Hagenmuller, J. Solid State Chem. 53 (1984) 387.
[9] J. Millet, M.M. Mentzen, Eur J. Solid State Inorg. Chem. 28 (1991) 493.
[10] G. Rousse, J. Rodríguez-Carvajal, C. Wurm, C. Masquelier, Solid State Sci. 4 (2002) 973.
[11] M. Gabelica-Robert, M. Goreaud, P. Labbe, B. Raveau, J. Solid State Chem. 45 (1982) 389.
[12] G.M. Sheldrick, SHELXS-97, University of Göttingen, Germany, 1997.
[13] G.M. Sheldrick, SHELXL-97: program for crystal structure refinement, University of Göttingen, Germany, 1997.
[14] I.V. Zatovsky, T.I. Ushchapivska, N.S. Slobodyanik, I.V. Ogorodnyk, Russ. J. Inorg. Chem. 51 (2006) 35.
[15] N. Ouerfelli, A. Guesmi, P. Molinie, D. Mazza, M.F. Zid, A. Driss, J. Solid State Chem. 180 (2007) 2942.
[16] E. Dvoncova, K.-H. Lii, J. Solid State Chem. 105 (1993) 279.
[17] M.-H. Whangbo, D. Dai, H.-J. Koo, Dalton Trans. (2004) 3019–3025.
[18] G.S. Gopalakrishna, B.H. Doreswamy, M.J. Mahesh, M. Mahendra, M.A. Sridhar, J. Shashidhara, K.G. Ashamanjari, Bull. Mater. Sci. 28 (2005) 1.